Recycled Poly(ethylene terephthalate)/Linear Low-Density Polyethylene Blends Through Physical Processing

Yue Zhang, Hongsheng Zhang, Yingbo Yu, Weihong Guo, Chifei Wu

Polymer Alloy Laboratory, School of Materials Science and Engineering, East China University of Science and Technology, Shanghai 200237, People's Republic of China

Received 4 July 2007; accepted 12 January 2009
DOI 10.1002/app.30030
Published online 17 June 2009 in Wiley InterScience (www.interscience.wiley.com).

ABSTRACT: Poly(styrene-ethylene/butylene-styrene) (SEBS) was used as a compatibilizer to improve the thermal and mechanical properties of recycled poly(ethylene terephthalate)/linear low-density polyethylene (R-PET/LLDPE) blends. The blends compatibilized with 0–20 wt % SEBS were prepared by low-temperature solid-state extrusion. The effect of SEBS content was investigated using scanning electron microscope, differential scanning calorimeter, dynamic mechanical analysis (DMA), and mechanical property testing. Morphology observation showed that the addition of 10 wt % SEBS led to the deformation of dispersed phase from spherical to fibrous structure, and microfibrils were formed at the interface between two phases in the compatibilized blends. Both differential scanning calorimeter and DMA results revealed that the blend with 20 wt % SEBS showed better compatibility between PET and LLDPE than other blends studied. The addition of 20 wt % of SEBS obviously improved the crystallizibility of PET as well as the modulus of the blends. DMA analysis also showed that the interaction between SEBS and two other components enhanced at high temperature above 130°C. The impact strength of the blend with 20 wt % SEBS increased of 93.2% with respect to the blend without SEBS, accompanied by only a 28.7% tensile strength decrease. © 2009 Wiley Periodicals, Inc. J Appl Polym Sci 114: 1187–1194, 2009

Key words: poly(ethylene terephthalate); linear low-density polyethylene; poly(styrene-ethylene/butylene-styrene); compatibilization; blends; compatibility; crystallization; morphology

INTRODUCTION

Poly(ethylene terephthalate) (PET) is a thermoplastic polyester widely used in the fields of fibers, films, and beverage packages. Historically, PET was rarely applied in engineering plastics because of the slow crystallizing speed and the sensitivity to charpy impact. However, these problems can be overcome by blending PET with other polymeric materials such as bisphenol, a polycarbonate (PC),[1–4] polyolefin (PO),[5–9] polyamide[10,11] liquid crystalline polymer,[12–14] and polyurethane.[15]

The modification of PET with PO to attain new materials with improved properties has recently attracted much interest, because of their relatively low cost and high performance. Moreover, the industrialization in producing new blends based on PET is beneficial to recycle waste PET. Many articles have been published on the blending of PET with various POs,[5–9,16–21] such as polypropylene (PP), high-density polyethylene, and low-density polyethylene (LDPE), but few articles have focused on linear LDPE (LLDPE).[5,22]

Because of the high immiscibility of PET and LLDPE, PET/LLDPE blend[5] shows a clear two-phase structure and poor mechanical properties. Therefore, the addition of suitable block or graft copolymer as compatibilizer is necessary to improve the compatibility of the blend. The copolymer should contain some segments that can interact with the segments in the respective PET and LLDPE phase,[23] thus giving rise to the preferential location at the interface between two phases.

Generally, recycled PET (R-PET) undergoes a series of degradation problems, such as thermal, hydrolytic, mechanical, and oxidative degradation during the melt processing.[24–27] It leads to the reduction of molecular weight and intrinsic viscosity of R-PET and hence a decrease in the mechanical properties of recycled materials.[24] For the extrusion of R-PET, it is important to develop a new technology to maintain its intrinsic viscosity and mechanical properties during processing.

In this work, LLDPE and poly(styrene-ethylene/butylene-styrene) (SEBS) were used to modify R-PET beverage bottle scraps. Blends of R-PET/LLDPE compatibilized with 0–20 wt % SEBS were extruded at the temperature below the melting temperature

Correspondence to: C. Wu (wucf@ecust.edu.cn).
Contract grant sponsor: National Natural Science Foundation of China; contract grant number: 20574019.

(T_m) of PET both at pre-zone and at die. We named this extrusion technology as low-temperature solid-state extrusion to distinguish from the other extrusion technology. In our previous work, low-temperature solid-state extrusion technology was investigated intensively.[1–3,5] At lower extrusion temperature, degradation of PET was improved effectively. The effects of SEBS as a compatibilizer on the morphology, thermal properties, dynamic mechanical properties, and mechanical properties of the blends were studied systematically.

EXPERIMENTAL

Materials and processing

Scraps of R-PET bottle were purchased from Zijiang Bottle (Shanghai, China) with an intrinsic viscosity of 0.71 dL/g. LLDPE was supplied by Panjin Polyethylene Industry Co., $T_m = 126.0$°C, MI = 2.72 g/10 min (265°C, 2.16 kg). SEBS (Kraton G1650) was from Shell Chemical Company with 70 wt % of ethylene–butylene block and 30 wt % of styrene block.

Scraps of R-PET were dried in dehumidifier at 120°C for 10 h. LLDPE and SEBS were dried under vacuum at 60°C for 10 h. Blends of R-PET/LLDPE/SEBS were prepared at a constant R-PET/LLDPE (4 : 1) ratio with SEBS contents of 0, 5, 10, 15, and 20 wt % with respect to the whole weight fraction of the blends. The reactive extrusion process experiments were implemented on a co-rotating twin-screw (L/D = 48, D = 35 mm). The barrel temperatures for the extruder from zone 1 to 4 were 100, 150, 200, and 230°C, respectively. The die temperature was 240°C. The extruded granules were dried in a dehumidifying dryer at 120°C for 4 h and injected to gain samples by injection molding at 240°C.

Characterization

Scanning electron microscopy (SEM) was carried out on JOEL model JSM 6100 instrument. Cryofractured or etched surfaces were coated with gold before testing and examined at a tilt angle of 30°. Tetrahydrofuran (THF) was used to remove SEBS. Warm xylene was used to remove both SEBS and LLDPE.

Differential scanning calorimeter (DSC) was performed on NETZSCH DSC PC 200 (German). The samples (7–10 mg), taken from the injection-molded specimens, were heated from 50 to 280°C in a nitrogen atmosphere, then cooled to 50°C, and reheated to 280°C in the second run at the constant heating/cooling rate of 10°C/min. Melting temperature, T_m, was determined according to the maximum of the endothermic curve.

Dynamic mechanical analysis (DMA) was determined using a Rheogel-E4000 DMA (Japan) at a fixed frequency of 1 Hz. Specimen dimensions were $40 \times 4 \times 2$ mm^3. The storage modulus (E'), loss modulus (E''), and loss tangent (tan δ) were obtained at a heating rate of 3°C/min as a function of temperature within the range from −130 to 230°C. All the measurements were carried out in a bending mode.

Tensile properties were tested by WSM-20KN Mechanical Properties Testing Machine, according to Chinese Standard GB/T1040-1992 at 23°C. Charpy impact strength was performed by JJ-20 Memorial Impact Tester, according to Chinese Standard GB/T 1043–1993 at 23°C. Both testing machines were manufactured by Changchun Mechanical Properties Testing Machine (China).

RESULTS AND DISCUSSION

Morphology

The ultimate goal of compatibilization is to achieve stable phase morphology and improved mechanical properties of the bends. The final mechanical properties depend greatly on the morphology of the blends. Figure 1 presents the SEM micrographs of the R-PET/LLDPE blends with and without SEBS. The noncompatibilized blend shows droplet dispersion type morphology, as seen in Figure 1(a). The dispersed LLDPE particles range in size from 2 to 6 μm. The smooth cavities and particles on the cryofractured surface reveal the poor interfacial adhesion between PET and LLDPE phase.

Figure 1(b–e) shows micrographs of the cryofractured surfaces for R-PET/LLDPE blends compatibilized with 5, 10, 15, and 20 wt % SEBS, respectively. It can be seen that the addition of SEBS results in higher phase dispersion with reduced particle sizes as compared with the noncompatibilized blends. With the addition of 10 wt % SEBS, LLDPE spherical droplets are deformed to fibrous structure. Further increasing SEBS leads to more uniform domain size and fewer cavities formed by the pullout of particles. The results indicate that the increase in SEBS content leads to better efficiency of SEBS in reducing the tendency of dispersed particles to coalesce, improving the interfacial adhesion between two phases and hence finer morphology of the blends.

It is well know that the localization of compatibilizer at the interface will promote the formation of finer and more stable morphology for the blends.[23] The etched surfaces for the blends of R-PET/SEBS and R-PET/LLDPE/SEBS are presented in Figure 2. R-PET/SEBS (70/30 w/w) blend was etched by THF at ambient temperature to remove SEBS. As shown in Figure 2(a), some microspheres adhere to the etched surface of the matrix. The etched surface of R-PET/SEBS (70/30 w/w) blend has been analyzed by Fourier transform infrared measurement before.

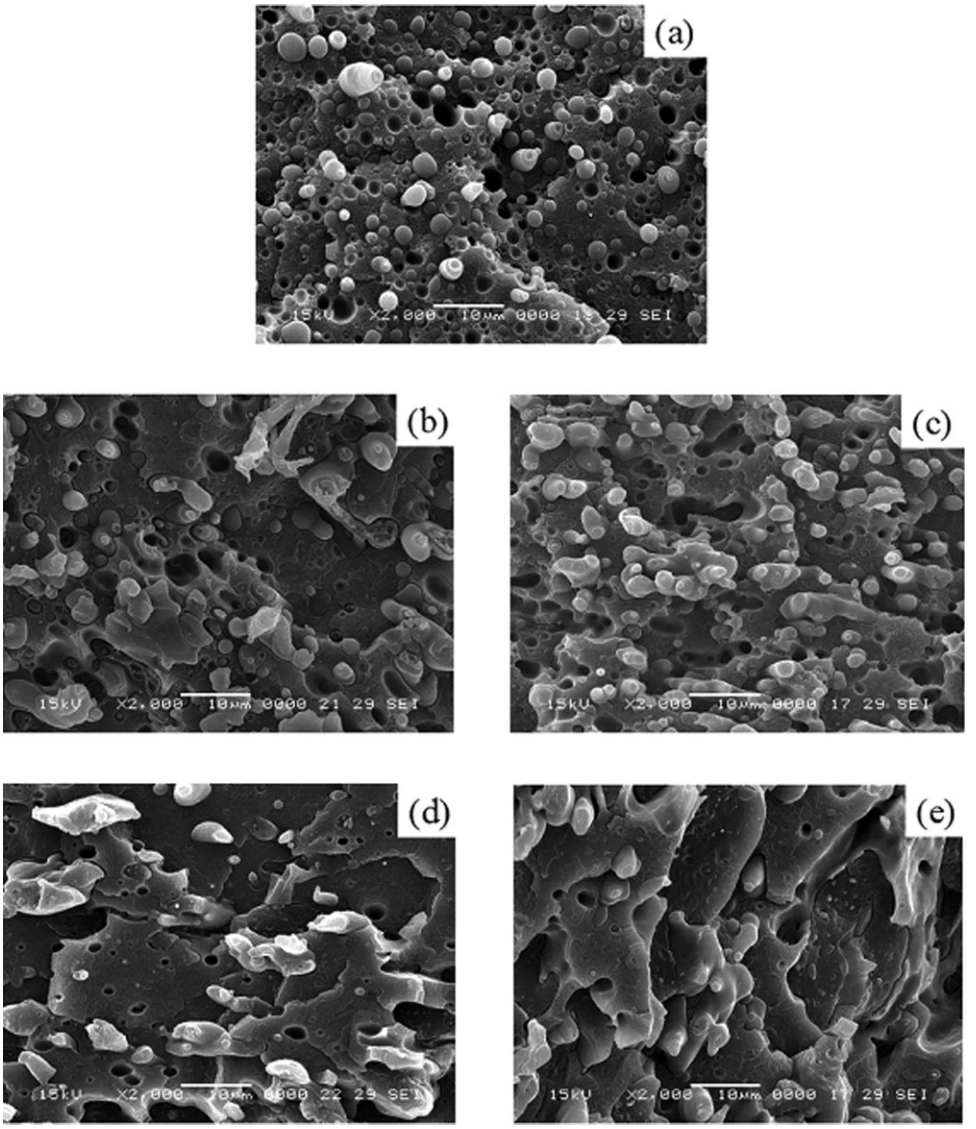

Figure 1 SEM micrographs of R-PET/LLDPE blends with and without SEBS.

The infrared spectra revealed the absorption band of SEBS. The R-PET/LLDPE/SEBS (64/16/20 w/w/w) blend was etched with the same method, and the etched surface is presented in Figure 2(b). It can be observed that lots of small particles appear at the etched surface of matrix. To remove SEBS and LLDPE simultaneously, R-PET/LLDPE/SEBS (64/16/20 w/w/w) blend was etched by xylene at 120°C. Some microspheres still adhere to the etched surface of matrix, as shown in Figure 2(c). According to the characterizations of the etched surface for R-PET/SEBS (70/30 w/w) blend, it can be inferred that due to the shearing action during extrusion some segments of SEBS penetrate into the matrix while other segments agglomerate at the surface of matrix. After the solvent is removed, the agglomeration of SEBS forms the microspheres at the surface of PET. In the ternary R-PET/LLDPE/SEBS blends, LLDPE cannot be removed with SEBS in THF, so many dispersed particles deposit on the surface of PET after etching. With further etching in xylene, the formation of insoluble microspheres at the surface of PET further confirms the penetration of some segments of SEBS into PET phase, i.e., the existence of interaction between SEBS and PET. Therefore, the partial compatibility between SEBS and LLDPE together with the interaction between SEBS and PET make SEBS can act as bridge to improve the interfacial adhesion between PET phase and LLDPE phase. The result is similar to what have been reported for PET/PP/SEBS by Heino et al.[28] Furthermore, R-PET/LLDPE/SEBS (72/18/10 w/w/w) blend was etched by THF at ambient temperature. As seen in Figure 2(d), removal of SEBS yields wide gaps surrounding the dispersed phase, indicating that most SEBS chains locate at the interface between two

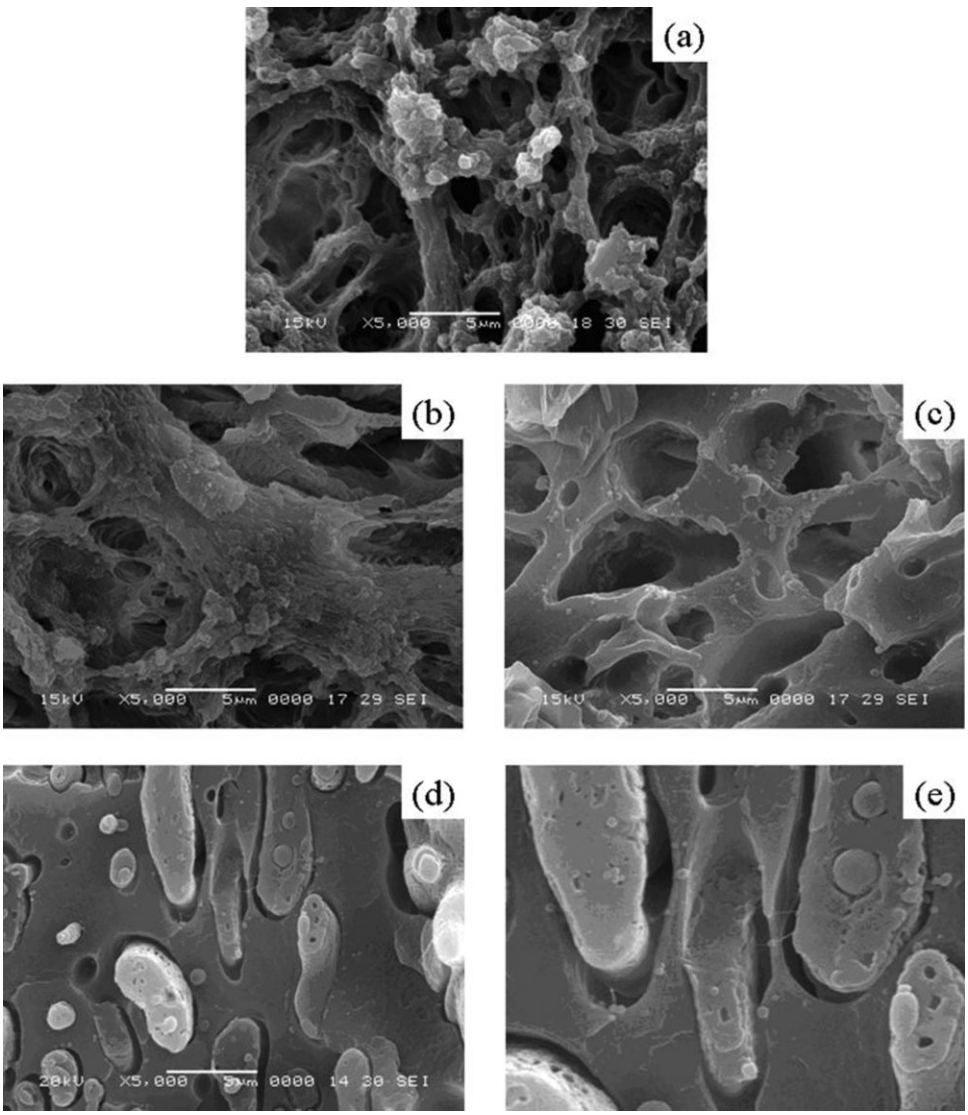

Figure 2 SEM micrographs of R-PET/SEBS and R-PET/LLDPE/SEBS etched blends.

phases. As the local enlargement of Figure 2(d), the formation of microfibrils between two phases is shown in Figure 2(e). It is the microfibril that leads to better interfacial adhesion and consequently finer morphology for the compatibilized blends.

Thermal behavior of PET

The DSC plots of R-PET/LLDPE blends with various contents of SEBS in the cooling and the second heating runs are shown in Figure 3 and Figure 4, respectively. The corresponding thermal data are listed in Table I. These results reveal that the addition of SEBS has more effect on the PET crystallization than the PET melting. R-PET/LLDPE/SEBS (64/16/20 w/w/w) blend exhibits the maximum value of crystallization temperature (T_c), and the minimum value of super-cooling temperature ($\Delta T = T_m - T_c$) and crystallization half-time ($t_{1/2}$) of PET.

$t_{1/2}$, defined as the time required for the degree of crystallinity to reach a level of 50%, was calculated by the following equation[29]:

$$t_{1/2} = \frac{T_{on} - T_{1/2}}{\varphi}$$

where T_{on} is the crystallization onset temperature where the thermograph initially departs from the base line, $T_{1/2}$ is the temperature where 50% of sample crystallinity has been attained, and φ is the cooling rate (°C/min). It is clear that the crystallization peak of PET is symmetric in Figure 3, so $T_{1/2}$ can be substituted by T_c of PET.

Both ΔT and $t_{1/2}$ represent the overall crystallization rate and were governed by rates of nucleation and growth. The lower is the ΔT or $t_{1/2}$, the higher is the crystallizibility. Compared with the binary PET/LLDPE blend, the compatibilized blends does

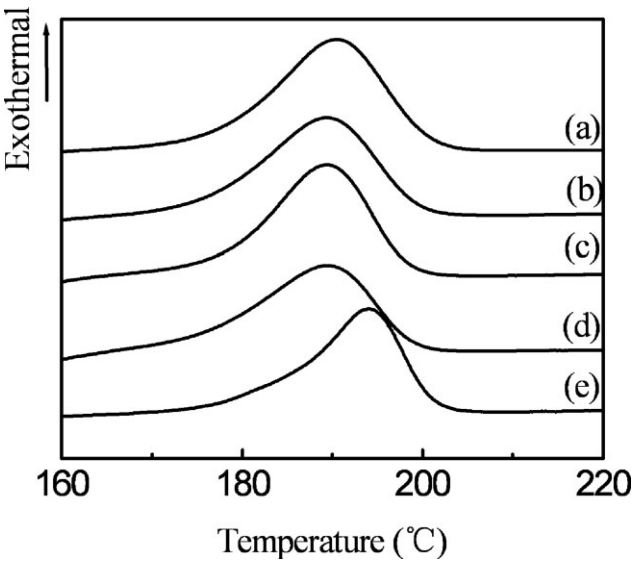

Figure 3 DSC plots of R-PET/LLDPE/SEBS blends (cooling scanning).

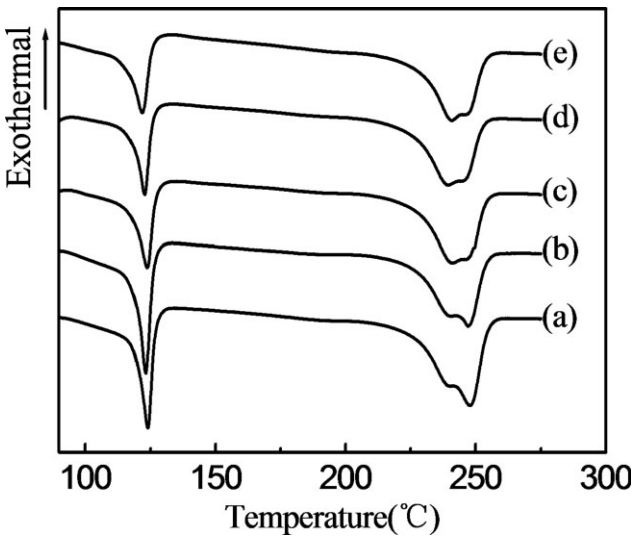

Figure 4 DSC plots of R-PET/LLDPE/SEBS blends (second heating scanning).

not show big changes in both ΔT and $t_{1/2}$ of PET until 20 wt % SEBS is added. For R-PET/LLDPE/SEBS (64/16/20 w/w/w) blend, ΔT and $t_{1/2}$ of PET decrease obviously, as seen in Table I. In addition, the crystallization rate was also defined as the crystallization enthalpy (ΔH_c) divided by the time from the onset to completion of crystallization ($\Delta H_c/t$).[28] It can be seen from Table I that the blend with 20 wt % SEBS shows the highest $\Delta H_c/t$ of PET ($\Delta H_c/t$ = 0.471 J g^{-1} s^{-1}). The results indicate that the crystallization rate of PET in the blend with 20 wt % SEBS is higher than that of PET in other blends. In this system, the addition of SEBS exerts two contrary effects on the crystallization of PET. On the one hand, the steric effect of SEBS hinders the ordered arrangement of PET chains on the surface of crystals. On the other hand, the compatibilization effect of SEBS facilitates the dispersion of LLDPE that can promote the crystallization of PET.[5] The highest crystallization rate of PET in the blend with 20 wt % SEBS suggests that the positive compatibilization effect obviously exceeds the negative steric effect because of the appropriate content of SEBS. The crystallization behavior of PET indicates that the compatibilization effect of SEBS on PET/LLDPE blends increases significantly with the increase in SEBS content from 5 to 20 wt %, which is agreement with the morphology observation.

In Figure 4, double melting peaks of PET are observed for all the blends. As seen in Table I, the addition of 5 wt % SEBS decreased the melting temperature (T_m), melting enthalpy (ΔH_m), and melting peak width (ΔT_m) of PET as compared with the noncompatibilized blend, but the T_m, ΔH_m, and ΔT_m of PET did not show further decrease with increase in SEBS content. The ΔT_m value is governed by the crystallite size distribution. The stable ΔT_m indicates that the crystallite size of PET is well distributed in the compatibilized blends, that is to say, SEBS content has no effect on the crystallite size distribution of PET.

Dynamic mechanical properties

The temperature dependence of storage modulus (E') and loss modulus (E'') for the R-PET/LLDPE blends with different content of SEBS are shown in Figures 5 and 6, respectively. The trend for E' and E''

TABLE I
DSC Data for R-PET/LLDPE Blends With and Without SEBS

SEBS content (wt %)	Melting (from the second heating scans)			Crystallization (from cooling scans)						
	T_m (°C)	ΔT_m (°C)	ΔH_m (J g^{-1})	$T_{c,on}$ (°C)	T_c (°C)	ΔT_c (°C)	$t_{1/2}$ (min)	ΔT (°C)	ΔH_c (J g^{-1})	$\Delta H_c/t$ (J g^{-1} s^{-1})
0	248.4	50.2	36.46	200.8	190.7	48.7	1.01	57.7	34.58	0.285
5	247.2	47.6	29.64	200.2	189.4	49.1	1.08	57.8	33.09	0.255
10	246.5	46.8	31.85	200.1	189.4	46.6	1.07	57.2	33.74	0.255
15	246.7	46.1	30.96	200.7	189.5	42.7	1.12	57.2	33.92	0.251
20	246.8	46.8	31.66	200.2	194.1	43.4	0.61	52.7	34.47	0.471

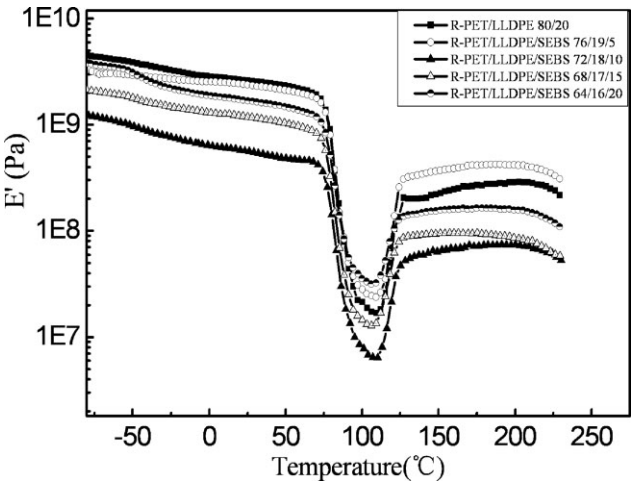

Figure 5 Storage modulus vs temperature of R-PET/LLDPE blends with and without SEBS.

of the blends with temperature increasing is similar. The abrupt drops of E' take place at about 70–110°C, because of the glass transition of PET. Then, a rapid increase in E' can be seen at above 110°C, corresponding to the cold crystallization of PET. When the temperature is above 130°C, the LLDPE phase transits to viscous state and the cold crystallization of PET is finished, so the E' value tends to be stable.

The E' of the blends decreases at first and then increase with the increase in SEBS content, and the minimum E' occurs at addition of 10 wt % SEBS. It can be explained that SEBS has two contrary effects on the E' of the blends in this system. One is the rubber nature of SEBS that decreases the E' of blends; the other is compatibilization effect of SEBS that improves the interfacial adhesion between two phases and thereby increases the E' of blends. At temperature below 110°C, the content of 5 wt % SEBS is too low to affect the properties of the blend, so E' of the blend with 5 wt % SEBS is comparable with that of the noncompatibilized blend. With addition of 10 wt % SEBS, the negative effect of rubber nature on decreasing the E' value becomes more and more significant. Unfortunately, 10 wt % SEBS is not sufficient to improve the compatibility of the blend obviously, leading to a progressive decrease in E' of the blend. With further increase in SEBS content, the obvious compatibilization effect results in much better adhesion between the phases, which overcomes partial decrease in E' caused by the rubber nature of SEBS, so E' of blend increases with the increase in SEBS content from 15 to 20 wt %. It can be seen from Figure 5 that the effect of SEBS content on the E' of blends at high temperature above 130°C is similar to that at low-temperature section, except for the addition of 5 wt % SEBS. The interaction between SEBS and other components increases with the increase in temperature, leading to further increase in interfacial adhesion between the phases. However, with the addition of more than 5 wt % SEBS, the increased interfacial adhesion is not enough to offset the negative rubber nature of SEBS. Therefore, only the blend with low content of SEBS shows higher E' than the noncompatibilized blend at high-temperature section.

The temperature dependence of the loss tangent (tan δ) of the blends is presented in Figure 7. The α-relaxation of LLDPE is far weaker than that of PET, so the T_g of LLDPE is not taken into account to investigate the compatibility of the blends in this article. For all the tan δ curves, a main peak appears at about 84.9–85.2°C, which corresponds to the glass transition temperature (T_g) of PET, and a weak transition appears at about 115°C, which is assigned to the cold crystallization temperature (T_{cc}) of PET. With the increase in SEBS content, almost no shifts

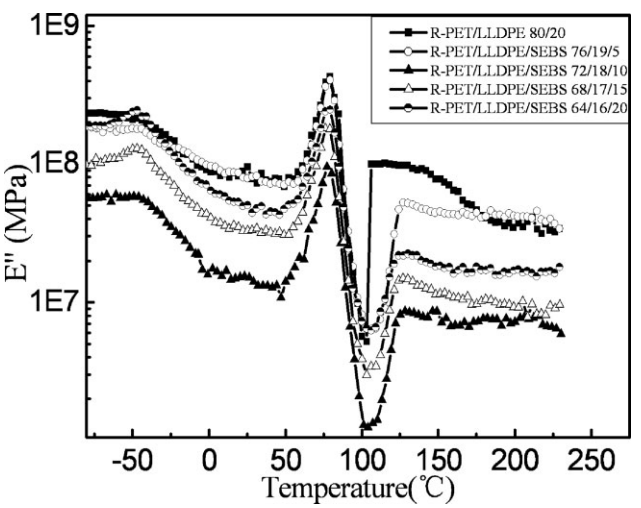

Figure 6 Loss modulus vs temperature of R-PET/LLDPE blends with and without SEBS.

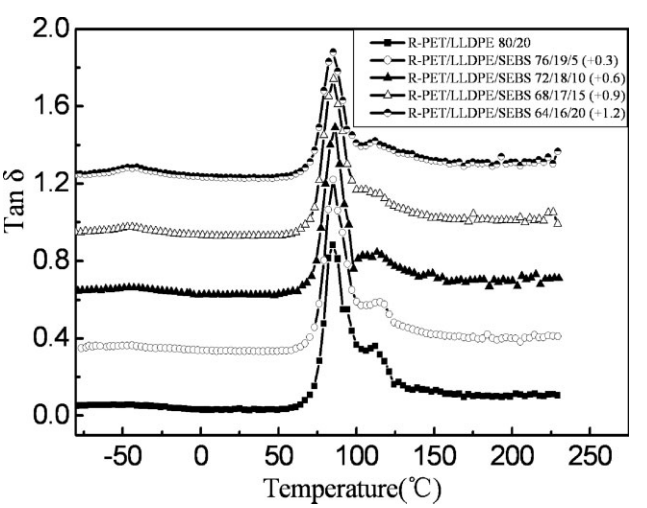

Figure 7 Loss tangent vs temperature of R-PET/LLDPE blends with and without SEBS.

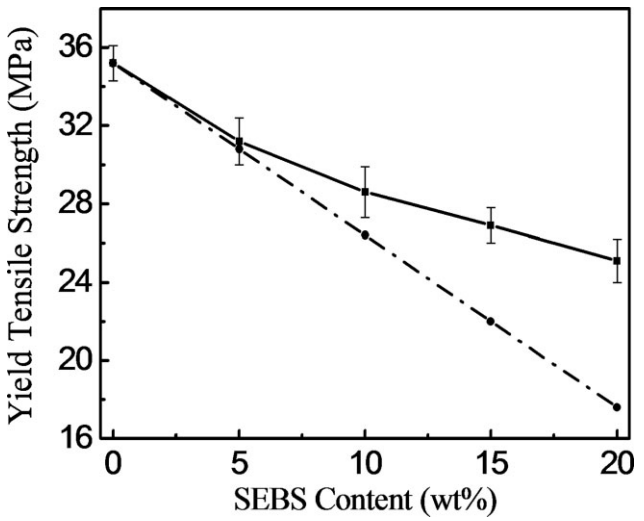

Figure 8 The effect of SEBS content on yield tensile strength of R-PET/LLDPE blends with and without SEBS.

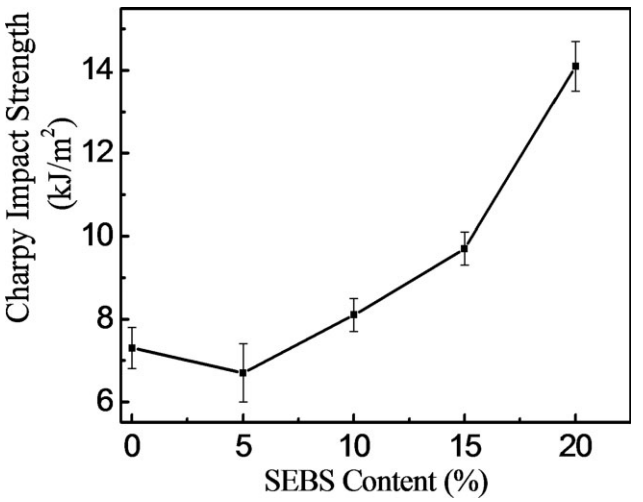

Figure 10 The effect of SEBS content on charpy impact strength of R-PET/LLDPE blends with and without SEBS.

of the peaks are observed, indicating that only a small amount of SEBS chains enter into the PET phase by physical interaction.

Mechanical properties

Figure 8 shows the yield tensile strength of R-PET/LLDPE blends as a function of SEBS content. Because of the rubber nature of SEBS, the yield tensile strength of the blends decreases from 35.2 to 25.1 MPa with the increase in SEBS content. However, the yield tensile strength of the compatibilized blends is higher than the predicted value, which is calculated according to the rule of mixtures, and deviates from the latter more and more seriously with the increase in SEBS content. It indicates that the addition of SEBS improves the interfacial adhesion between the matrix and the dispersed phase and consequently promotes the applied stress to transfer across the interfaces effectively.

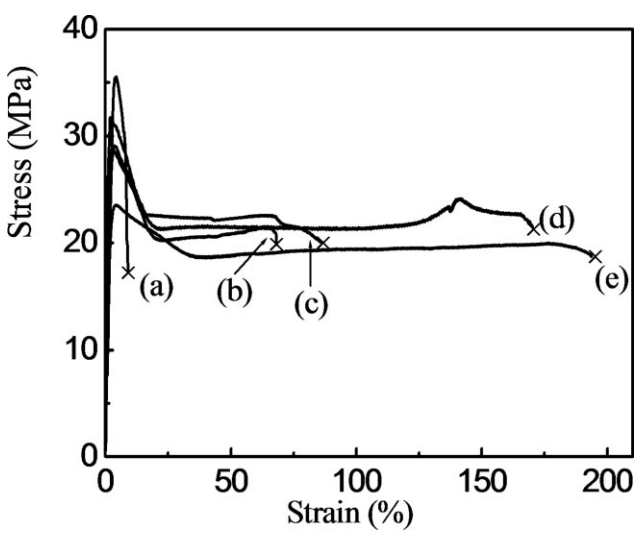

Figure 9 The effect of SEBS content on terminal elongation of R-PET/LLDPE blends with and without SEBS.

Figure 9 depicts the strain–stress curves of blends during tensile testing. For the noncompatibilized R-PET/LLDPE blend, the elongation at break is only 10.4%. With the addition of SEBS, the elongation at break of the blends increases obviously. The elongation at break of 182% is obtained for the blend with 20 wt % SEBS. This is due to the more stable morphology with finer dispersion of the LLDPE phase and better interfacial adhesion between the phases in the compatibilized blends. As a result, the brittle fracture is inhibited and more microcracks are formed under applied stress.

Figure 10 shows the charpy impact strength of R-PET/LLDPE blends as a function of SEBS content. The compatibilized blends show higher impact strength than the binary R-PET/LLDPE blend (7.3 kJ/m^2). With the addition of 20 wt % SEBS, the charpy impact strength of blends increases to 14.1 kJ/m^2. It indicates that the addition of SEBS promotes more energy to be absorbed and dissipated in the impact test. However, for the R-PET/LLDPE with 5 wt % SEBS, only few SEBS chains locate at the interface to improve the adhesion between two phases. Because of the weak compatibilization effect, the addition of 5 wt % SEBS has little effect on the charpy impact strength.

CONCLUSIONS

In this work, R-PET/LLDPE blend compatibilized with SEBS through physical processing were investigated. SEM observation showed that the addition of

SEBS resulted in more stable and uniform morphology. With the addition of 10 wt % SEBS, the spherical droplets of LLDPE were deformed to the fibrous structure. The micrographs of etched surface of the blends indicated the existence of interaction between SEBS and PET as well as the formation of microfibrils between PET and LLDPE phase.

DSC results revealed that the addition of 5–15 wt % SEBS had no effect on the crystallization behavior of PET, whereas the blend with more than 15 wt % of SEBS showed an obvious increase in crystallization rate of PET. The better compatibility of the blends with 20 wt % SEBS caused the maximum $\Delta H_c/t$ and minimum $t_{1/2}$ of PET. The addition of 5 wt % SEBS decreased the T_m, ΔH_m, and ΔT_m of PET, but further increasing of SEBS content had no effect on the melting behavior of PET.

DMA analysis showed that the addition of more than 10 wt % SEBS inhibited the decrease in E' caused by the rubber nature of SEBS, indicating that the interfacial adhesion between two phases was improved obviously at SEBS content above 10 wt %. It was also shown that the interaction between SEBS and other components enhanced at high temperature. No shift in the T_g of PET with the increase in SEBS content pointed out that only few SEBS chains entered into the matrix by physical interaction.

When SEBS was added to the binary blend, the elongation at break and impact strength of the blends increased obviously, and the yield tensile strength did not decrease linearly. With the addition of 20 wt % SEBS, the elongation at break and impact strength increased to 182% and 14.1 kJ/m^2, respectively. The improved mechanical properties lead to the conclusion that SEBS really acts as a compatibilizer between PET and LLDPE.

References

1. Guo, W. H.; Tang, X. W.; Yin, G. R.; Gao, Y. J.; Wu, C. F. J Appl Polym Sci 2006, 102, 2692.
2. Tang, X. W.; Guo, W. H.; Yin, G. R.; Li, B. Y.; Wu, C. F. Polym Bull 2007, 58, 479.
3. Guo, W. H.; Zhang, H. S.; Yin, G. R.; Tang, X. W.; Li, B. Y.; Wu, C. F. Polym Adv Technol 2007, 18, 551.
4. Vladimir, N. I.; Claudio, C.; Vittorio, T.; Roberto, P.; Francesco, P.; Corrado, B.; Maurizio, T.; Maurizio, F. Polymer. 1996, 37, 5883.
5. Zhang, H. S.; Guo, W. H.; Yu, Y. B.; Li, B. Y.; Wu, C. F. Euro Polym J 2007, 43, 3662.
6. Pietrasanta, Y.; Robin, J. J.; Torres, N.; Boutevin, B. Macromol Chem Phys 1999, 200, 142.
7. Kim, D. H.; Park, K. Y.; Suh, K. D. JMS—Pure Appl Chem 2000, 37, 1141.
8. Park, S. H.; Park, K. Y.; Suh, K. D. J Polym Sci Part B Polym/Phy 1998, 36, 447.
9. Kalfoulou, N. K.; Skafidas, D. S.; Kallitsis, J. K.; Lambert, J. C.; Stappen, L. V. Polymer 1995, 36, 4453.
10. Huang, Y. Q.; Liu, Y. X.; Zhao, C. H. J Appl Polym Sci 1998, 69, 1505.
11. Evatatiev, M.; Schultz, J. M.; Petrovich, S.; Georgiev, G.; Fakirov, S.; Friedrich, K. J Appl Polym Sci 1998, 67, 723.
12. Albert, B.; Alois, H. A. T. J Appl Polym Sci 1999, 71, 1125.
13. Pan, L. H.; Liang, B. R. J Appl Polym Sci 1998, 70, 1035.
14. Chin, H. C.; Chiou, K. C.; Chang, F. C. J Appl Polym Sci 1996, 60, 1503.
15. Samios, C. K.; Gravalos, K. G.; Kalfoglou, N. K. Euro Polym J 2000, 36, 937.
16. Pawlak, A.; Morawiec, J.; Pazzagli, F.; Pracella, M.; Galeski, A. J Appl Polym Sci 2002, 86, 1473.
17. Pracella, M.; Rolla, L.; Chionna, D.; Galeski, A. Macromol Chem Phys 2002, 203, 1473.
18. Kim, D. H.; Park, K. Y.; Kim, J. Y.; Suh, K. D. J Appl Polym Sci 2000, 78, 1017.
19. Champagne, M. F.; Huneault, M. A.; Row, C.; Peyrel, W. Polym Eng Sci 1999, 39, 976.
20. Cho, H. H.; Kim, K. H.; Kang, Y. A.; Ito, H.; Kikutani, T. J Appl Polym Sci 2000, 77, 2254.
21. Yoon, K. H.; Lee, H. W.; Park, O. O. J Appl Polym Sci 1998, 70, 389.
22. Retolaza, A.; Eguiazábal, J. I.; Nazábal, J. J Appl Polym Sci 2003, 87, 1322.
23. Paul, D. R.; Newman, S. Polymer Blends, Academic Press: New York, 1978; p 2.
24. Girija, B. G.; Sailaja, R. R. N.; Madras, G. Polym Degrad Stab 2005, 90, 147.
25. Paci, M.; La Mantia, F. P. Polym Degrad Stab 1998, 61, 417.
26. Sammon, C.; Yarwood, J.; Everall, N. Polym Degrad Stab 2000, 67, 149.
27. Botelho, G.; Queirós, A.; Liberal, S.; Gijsman, P. Polym Degrad Stab 2001, 74, 39.
28. Heino, M.; Kirjava, J.; Hietaoja, P.; Seppälä, J. J Appl Polym Sci 1996, 65, 241.
29. Qu, C. F.; Ho, M. T.; Lin, J. R. J Polym Res 2003, 10, 127.